JOINT EUROPEAN TORUS JET

JET-P(89)55

J.M. Adams, B. Balet, S. Conroy , J.G. Cordey, T. Elevant, R.D. Gill,
O.N. Jarvis, M.J. Loughlin, W. Mandl, P. D. Morgan, D. Pasini, G. Sadler,
P. van Belle, M. von Hellerman, N. Watkins and H. Weisen

Determination of Deuterium Concentrations in JET Plasmas

Determination of Deuterium Concentrations in JET Plasmas

J.M. Adams[1], B. Balet, S. Conroy[2], J.G. Cordey, T. Elevant[3], R.D. Gill, O.N. Jarvis, M.J. Loughlin, W. Mandl, P. D. Morgan, D. Pasini, G. Sadler, P. van Belle, M. von Hellerman, N. Watkins[1] and H. Weisen

JET Joint Undertaking, Culham Science Centre, OX14 3DB, Abingdon, UK

[1]*Harwell Laboratory, UKAEA, Oxon, OX11 ORA, UK*
[2]*Imperial College of Science, Technology and Medicine, London, SW7 2BZ, UK*
[3]*Royal Institute of Technology, Stockholm, Sweden*

Preprint of a paper to be submitted for publication in
Nuclear Fusion

ABSTRACT.

The concentration of deuterium in JET plasmas, expressed as a fraction of the electron concentration, has been determined using eight different methods, four of which involve neutron detection. The results from these various methods are found to be consistent within their experimental errors. The ratio n_D/n_e, measured at the moment of peak neutron emission strength, is found to lie in the range from nearly unity, for discharges into which deuterium pellets are injected, down to values of 0.4 or less for some of the highest performance discharges. Thisfinding is based on the analysis of discharges run in 1988, when the plasma-facing components within the vacuum vessel were of carbon or were carbon coated.

1. INTRODUCTION

The progress of nuclear fusion research is customarily assessed through the comparison with the fusion product needed for a fusion reactor, $n_D \tau_E T_i = 5 \times 10^{21} m^{-3}$ keV sec, where n_D is the fuel density, τ_E is the energy confinement time and T_i is the ion temperature. In practice, the electron density n_e is frequently substituted for n_D in this expression because it is the more easily measured quantity. However, with the operation of the large tokamaks (JET and TFTR) with high additional heating powers and, consequently, high T_i values, it has been found that the impurity influx into these plasmas can be very significant. Obviously, the purity of tokamak plasmas is one of the most important attributes, yet the accurate quantitative assessment of plasma species remains a challenging task. The purpose of this paper is to show that the fuel concentration (expressed as the ratio n_D/n_e) can be assessed by a variety of techniques and that the results from these techniques are consistent within their respective experimental errors. One conclusion is inescapable: most JET plasmas have disturbingly high impurity levels. This finding is based on the analysis of discharges run in 1988, when the plasma-facing components within the vacuum vessel were of carbon or were carbon coated; specifically, the 1989 operation with beryllium gettering has not yet been assessed.

The deuterium ion density in a tokamak plasma is not a directly measured quantity. It is usually derived from a knowledge of the main plasma impurities and a measured value of the effective ion charge, Z_{eff}. The central value of Z_{eff} can be found from the neoclassical plasma resistivity [1] for steady-state conditions as well as from X-ray pulse-height analysis [2]. On JET, a radial profile of Z_{eff} is deduced through an Abel inversion of the line-integrated measurement of visible bremsstrahlung emission obtained using a multi-chord array [3]; interestingly, this measurement has shown that the radial profile of Z_{eff} is not flat. Direct measurements of the major impurities in JET, carbon and oxygen, have recently become possible through the use of the charge-exchange recombination spectroscopy diagnostic [4-6] which determines the density and temperature profiles whenever the neutral beam injectors are operational, either as the heating source or as a probe, and so can supply the fast neutrals involved in the charge-exchange process.

More direct experimental techniques for determining the deuterium ion

densities are available through the study of fusion reaction rates and fusion reaction product energy spectra. These properties are determined by the velocity distributions and densities of the interacting ions. Depending on the plasma discharge conditions, the fusion reactions can be exploited in several different ways. In the case of plasmas in thermal equilibrium, the velocity distributions are determined by the ion temperature which, in JET, is routinely measured using a variety of techniques, so that a knowledge of the reaction rates allows the deuterium ion density to be determined [7]. For other cases of current interest, involving neutral deuterium beam injection [8] and the study of tritons emitted from d-d fusion reactions [9], the source velocity distributions can be considered to be known [10] and the slowing down distributions are determined by Coulomb collisions. Thus, measurements of the t-d and d-d fusion reaction rates once more determine the effective deuterium density, although in the latter case the neutron energy spectrum is additionally needed to determine the fraction of the neutron emission that is thermonuclear as distinct from being of beam-plasma interaction origin. Since the fusion reaction rates are normally strongly peaked at the centre of the plasma, the density measured by the these methods will be essentially the central density. However, there are exceptions to this rule, especially for H-mode discharges [11] for which the neutron emission radial profile can be quite flat (see below), so that care should be taken with the interpretation of the data.

2. DIAGNOSTIC TECHNIQUES FOR DETERMINING Z_{eff}

The various techniques for assessing the effective charge, Z_{eff}, in JET are listed in Table I; they are very briefly reviewed below. Some are more direct than others in that they require little data from other diagnostics or they rely on fewer plasma physics assumptions. In the present section, the uncertainties in the Z_{eff} measurements are quoted. For a plasma containing only deuterium and carbon, $n_D/n_e = 1-(Z_{eff}-1)/5$. The fractional uncertainty in the n_D/n_e value derived from Z_{eff} is given by

$$\delta(n_D/n_e)/(n_D/n_e) = -(\delta Z_{eff}/ Z_{eff})/(6/ Z_{eff}-1)$$

and is small for low Z_{eff} but very large for high Z_{eff}.

i) Visible Bremsstrahlung

The determination of Z_{eff} from the visible bremsstrahlung radiation [3] is only possible if the electron density and temperature profiles and the plasma geometry are available. Single horizontal and vertical chord

measurements are routinely made. A 15 chord array is also used to provide a Z_{eff} profile. This profile is typically peaked on-axis in the steady-state for most operating conditions but for H-modes it can be peaked off-axis, as shown in fig.1. The deduction of a line-averaged Z_{eff} is quite sensitive to the shape and absolute level of the electron density profile. This is the main reason for the estimated systematic errors being of the order of ±30%. The n_D/n_e ratio is derived from Z_{eff} by making the customary assumption for JET that the main plasma impurities are carbon and oxygen in the proportions 3:1. The uncertainty associated with n_D/n_e can be appreciable for fuel concentrations below 0.5.

ii) Plasma Resistivity

The resistive Z_{eff} is derived from the measured loop voltage, the electron temperature profile and the plasma geometry. The calculation [1] is only accurate when the plasma is in the steady state and when all non-inductively driven sources of current are small, when the typical error on this measurement of Z_{eff} will be ±25%.

A detailed comparison of the resistive Z_{eff} with the horizontal bremsstrahlung measurement for steady-state ohmically heated plasmas shows agreement within the errors of these measurements, although the data show quite a lot of scatter. The bremsstrahlung data are typically about 20% lower than the resistivity data, a difference which can be explained by the adoption of a flat Z_{eff} profile for routine calculations, whereas an on-axis peaking of up to 30% may be present for ohmic discharges.

iii) Pulse Height Analysis

A measurement of the soft X-ray energy spectrum intensity together with a knowledge of the electron density and temperature profiles provides a further estimate of Z_{eff} [2]. The errors on this evaluation of Z_{eff} are quite large, up to ±50%. The PHA values of Z_{eff} are systematically higher than the chord-averaged visible bremsstrahlung values but agree rather better with the central values, as would be expected owing to the strong central weighting of the PHA measurement.

iv) Charge-Exchange Recombination Spectroscopy

This diagnostic [4] provides radial profile measurements defined by the intersections of 15 viewing chords with the paths of the neutral beams from the injectors. It is usually tuned to the major plasma impurity, carbon. The resulting carbon density measurements are subject to an overall calibration uncertainty of about ±30%, traceable to the basic charge-exchange

cross-sections. A Z_{eff} radial profile derived from the carbon density is shown in fig.1 for comparison with the visible bremsstrahlung measurement; except at very large radius, the agreement is excellent.

The charge-exchange recombination spectroscopy (CXRS) diagnostic can also provide a direct local measurement of Z_{eff} through the analysis of the excited neutral beam Balmer-Alpha spectrum [5,6]; this requires no absolute calibration and is independent of electron density. The technique utilizes the ratio of the intensity of the D_α spectrum from the fast injected deuterium neutrals to that from the thermal plasma deuterons. The estimated error on the resulting Z_{eff} values is ±15%. Unfortunately, these measurements are only now becoming routinely available.

The CXRS technique permits the rapid changes in the carbon radial profiles and, consequently, the n_D/n_e profiles to be examined for full-power neutral beam-heated discharges. An example of this behaviour is shown in fig. 2 for an H-mode discharge (formed in a magnetic X-point configuration) where the change from a flat L-mode profile to a hollow H-mode profile can be seen.

3. NEUTRON ESTIMATES OF DEUTERIUM CONCENTRATION

Different neutron measurement techniques (Table I) can be applied as the plasma conditions are varied; the simplest situation is for ohmic and ICRF heating, neutral beam heating is rather more complicated, neutral beam injection transient analysis constitutes a special case and the examination of triton burnup requires high neutron emission strengths. Not only do these neutron techniques have to be applied with some degree of circumspection with regard to plasma operating conditions but due regard must be paid to their very novelty. As an example of the former, it should be recognized that high power ICRF heating tuned to hydrogen gives rise to a weak component of energetic deuterons through second harmonic acceleration; the absence of these high energy deuterons must be demonstrated before the data can be reliably analyzed.

i) Neutron Emission Profile Analysis (Ohmic and ICRF heating)

For this case, the plasma is assumed to be in thermal equilibrium, the magnetic flux surfaces being contours of neutron emission strength. The central ion temperature is obtainable from several diagnostics including Neutron Spectrometry [14], Nickel X-ray Crystal Spectroscopy [15] and Neutral Particle Analysis [16]. According to availability, a suitable average of these measurements is taken. The 2.5 MeV neutron emission radial profiles are routinely recorded with the 19-channel Neutron Profile Monitor [17]. A

computer code (ORION, [17]) is used to reproduce the experimental line-integrated count-rates by adjusting a parametrized neutron source profile to the data using a maximum likelihood technique. For this purpose, the deuterium density profile is assumed to be the same as the electron density profile as given by the Interferometer [12] or Lidar [13] diagnostics. An initial estimate of the central deuterium density is obtained from the axial value of Z_{eff}; this density is then iterated until the central ion temperature obtained from ORION reproduces the measured value. For convenience, the density is presented as the ratio n_D/n_e; the estimated accuracy is about ±20%.

ii) Neutron Energy Spectra and Emission Profile Analysis (NBI discharges)

The 2.5 MeV neutron energy spectrum for the central region of the JET plasma is measured using a double-interaction time-of-flight neutron spectrometer [18]. The neutron energy spectra contain two components, a contribution from thermal (plasma-plasma) reactions and a contribution from beam-plasma reactions. As is well-known, the thermal contribution is Gaussian with its width approximately proportional to $T_i^{0.5}$. The beam-plasma contribution is more complicated with a shape which depends on geometry and beam injection energy; it is calculated using the kinematics code FPS [10]. With the shapes of the two contributions known, it is a relatively straightforward matter to adjust their relative proportions until a good fit to the measured spectrum is obtained, as demonstrated in ref.8. In this manner, we derive the thermal to total neutron production ratio. At this point, we have sufficient information to invoke the code ORION and to deduce the central density ratio (to ±25%) as was done for ohmic discharges. It should be noted that this derivation is only approximate. A more rigorous analysis would take account of the fact that for beam-heated discharges the magnetic flux surfaces are not contours of neutron emission strength. Also, the present approach is to assume that the radial profiles for thermal and beam-plasma neutron emission are the same. For most discharge conditions, this is a good working hypothesis; however, for high plasma current H-mode discharges the assumption may introduce non-negligible errors.

iii) Neutral Injection Transient Analysis

This technique exploits the fact that the change in neutron emission strength at beam switch-on (which is abrupt) is entirely due to beam-beam and beam-plasma interactions and is principally dependent on the beam power, beam energy and deuterium concentration (n_D/n_e), and is only weakly dependent on electron and ion temperatures. The time-dependent code TRANSP [19] is used to force agreement between measurement and prediction just after switch-on time

by adjusting the n_D/n_e ratio. This provides a normalization factor for the Z_{eff} value obtained from measurements of the visible bremsstrahlung; whenever available, the radial profile of Z_{eff} is utilized. The adjusted Z_{eff} is found to have the correct time evolution to provide acceptable agreement between calculated and measured neutron emission strengths for all later times in the discharge. The accuracy of the (n_D/n_e) estimate is typically ±20%. Only selected discharges have been studied with TRANSP as it is a highly cpu-intensive code.

iv) Triton Burnup

The 14 MeV neutron emission from JET discharges can be studied by a combination of techniques. The absolute magnitude of the 14 MeV neutron emission is obtained from neutron activation measurements [20], using a pneumatic transfer system to place capsules containing suitable materials close to the plasma edge. A silicon diode technique provides the time evolution [9,21]. The triton burnup study is normally oriented towards testing whether or not the slowing down and fusion reaction rates of the 1.0 MeV tritons emitted from d-d reactions can be correctly predicted using standard procedures. For this purpose, it is necessary to restrict the discharges to be studied to the rather sparsely populated class of low Z_{eff} discharges. In the present application, we invert the usual approach by assuming the standard calculation procedures to be verified by this work, in which case forcing agreement between prediction and calculation provides a measurement of the n_D/n_e ratio to an accuracy of about ±20%. This method is expected to be of most value when Z_{eff} is rather high (e.g.≥3).

4. COMPARISON OF n_d/n_e VALUES

Most of the diagnostic techniques described above provide data on a routine basis, i.e. for every discharge, but the data analysis can be difficult and often relies on the prior analysis of data from other diagnostics. Thus, only a small selection of discharges can be analyzed in full. Accordingly, we have chosen to investigate a number of discharges from the 1988 period of operation, selected so as to cover a broad range of discharge conditions.

Before discussing the detailed results, a brief account of the present understanding of impurity levels will be given. First, we note that all plasma-facing components in JET are either constructed from graphite or are carbon-coated so that carbon is expected to be present in significant

quantities. It appears that the discharge is formed initially as a reasonably high purity plasma (except at low densities); the steady-state impurity level is determined by the plasma edge temperature, which in turn is usually related to the central temperature. Early work with neutron spectrometry [7] indicated that the n_D/n_e ratio falls with increasing central temperature for ohmic discharges, but that this fall is not further enhanced by the addition of low power ICRF heating, presumably because the RF heating is central and therefore does not greatly affect the edge conditions.

Additional heating is not normally applied until steady-state plasma conditions are achieved; discharges heated during the current-rise phase form a special case which will be considered below. Up to 20 MW of either NBI or ICRF power are available but when the heating mechanisms are combined it is found that only up to 10 MW of ICRF power can be coupled into the plasma. The "carbon catastrophe" encountered with high-power NBI heating is shown clearly in fig.3, where the central carbon density as measured by charge-exchange recombination spectroscopy is compared with the neutron emission strength as a function of time into the discharge. The carbon density at the edge begins to rise just after beam switch-on time and penetrates to the centre after a delay of 0.5 to 1 second. Once the carbon reaches the centre, the neutron emission strength begins to fall rapidly. Neutral beam injection of deuterium is expected to fuel the plasma; clearly, it does so at first but soon cannot compete with the carbon influx. A similar effect may occur when high-power ICRF heating is applied but the effects are less pronounced. It has been noted that the performance of combined heating has been rather disappointing in that the neutron emission strength is frequently reduced rather than increased by the addition of high ICRF power; this is presumably because, for operational reasons, the ICRF power was ramped up over a period of 1 second, which is just sufficient for the raised impurity influx to reach the centre before the NBI was applied. It was further discovered that edge fuelling with a sequence of short penetration deuterium pellets during the heating phase improved the n_D/n_e ratio; this can be interpreted as a consequence of a reduction of plasma edge temperature rather than of fuel diffusing to the plasma centre.

Whilst the normal trend is for the deuterium concentration factor to be disturbingly low, especially when high additional heating powers are applied, there was one sequence of high power ICRF heated discharges which is worthy of note because the concentration ratios were close to unity without the intervention of pellet fueling. For this sequence, the vacuum vessel was well-conditioned, with ohmic discharges in ^4He being interspersed between the normal discharges to help maintain that condition. An additional factor was the high central electron density ($n_e \sim 6\times10^{19}$ m^{-3}) attained during the

RF-heated period. When the RF heating was applied during the plasma current-rise phase (before the onset of sawtooth oscillations), the concentration ratio obtained from the neutron emission analysis (ORION) was about 0.8, this being maintained until the first sawtooth crash after which it fell to about 0.65. By way of contrast, when the RF heating was applied during the plasma current flat-top phase the concentration ratio was 0.65 during the RF-heated period, falling to 0.55 for the subsequent ohmic heating period. These observations are in accord with the understanding that the transport of impurities to the plasma centre is facilitated by sawtooth oscillations. Possibly as a consequence of the impurity levels, the heating effectiveness of the RF was greater during the current-rise phase than during the flat-top period, with central temperatures of 6 keV as opposed to 4 keV, respectively, being recorded by neutron spectrometry. A potential complication of high power RF heating when tuned to hydrogen as the minority ion species is the generation of an energetic tail to the ion energy distribution which could be responsible for the production of a large fraction of the observed neutron yield; examination of the neutron energy spectra showed that this contribution never exceeded 20% when averaged over the usual 1-second sampling period required by the neutron spectrometer.

The important parameters of the discharges selected are presented in Table II; the discharges are placed in groups which correspond to the feature identified as being of most interest and the quoted plasma parameters correspond to averages over the period of 0.5 sec or more during which the neutron emission strength remains close to its maximum value. The different measurements of Z_{eff} are reported in Table III. Note that Abel-inverted electron density profiles are required for the visible bremsstrahlung analysis of H-mode discharges; for all other conditions a parabolic density profile prescription can be adopted. Only the line-averaged visible bremsstrahlung values for Z_{eff} are routinely available. The PHA-derived values for $Z_{eff}(0)$ agree within the rather large errors with the central bremsstrahlung value. The $Z_{eff}(0)$ values derived from the charge-exchange measurement are compatible with the other values. For comparison purposes, the charge-exchange profile data are transformed into line-averaged values with similar weightings to the visible bremsstrahlung measurement; the agreement between the two sets of values is good.

As already noted, carbon and oxygen impurities are known to be present in significant quantities and must be taken into account when deducing the deuterium densities. Additionally, there may be hydrogen or ^{3}He intentionally introduced at the 5 to 10% level to act as minority ion for the ICRF heating. Also, ^{4}He is occasionally employed for clean-up discharges (to extract

absorbed deuterium from the vessel walls prior to running low density discharges), after which it is sometimes used as prefill gas with deuterium being puffed in later. The precise quantities of these light ions in the plasmas are not well diagnosed so that the deuterium densities deduced from Z_{eff} are likely to be over-estimates.

Table IV lists the n_D/n_e ratios deduced from the four neutron measurement methods and compares them with the value derived from the appropriate axial Z_{eff} measurement, taken to be the average of the visible bremsstrahlung and charge-exchange measurements where both are available, or the surviving measurement otherwise. It is important to note that the n_D/n_e ratio derived from a neutron spectrum represents a central measurement and is usually in good agreement with the central Z_{eff} value. However, the present form of analysis is likely to be over-simplified for the H-mode discharges as these can have very flat, if not hollow, density and fusion reactivity profiles. The bulk of the neutron production for these discharges originates from regions situated at 0.3 to 0.4m from the axis and therefore the triton burnup and TRANSP analysis n_D/n_e values for H-mode discharges are rather lower than the central values. It is, of course, these rather than the central values which characterize the fusion reactor prospects for such discharges.

The results given in Table IV are presented graphically in fig. 4, where the averages of the neutron neutron-based measurements are taken, except for the H-mode discharges, for which the axial values are utilized. It is seen that the agreement between the bremsstrahlung measurements and the neutron measurements is quite acceptable. It is particularly gratifying that the analysis of the centrally pellet fuelled discharges should have produced density ratios close to unity; these discharges can be taken as helping to validate the neutron spectrometry technique for ICRF and combined heating scenarios. Unfortunately, it appears that the neutron yields from the highest performance discharges are usually restricted by high impurity levels.

5. CONCLUSIONS

A representative selection of discharges from the operation of JET during 1988 has been studied. The various measurements of Z_{eff} are compared in Table III, and the n_D/n_e values derived from the visible bremsstrahlung data are compared with the neutron values in Table IV. The time intervals under investigation were those corresponding to the maximum neutron emission strengths for the discharge in question. The following conclusions can be drawn:

(i) The several measurements of Z_{eff} agree within their experimental

errors.

(ii) The neutron measurements agree within their respective errors.

(iii) The visible bremsstrahlung estimate of n_D/n_e is in broad agreement with the neutron assessment.

(iv) The deuterium concentration ratio is found to range from nearly unity for discharges into which deuterium pellets are injected, down to values of 0.4 or less for some of the highest performance discharges.

REFERENCES

[1] J P Christiansen, "Integrated Analysis of Data from JET", JET-R(86)04

[2] D Pasini et al, Rev. Sci. Instrum. 59 (1988) 693.

[3] P D Morgan, 15th European Conference on Controlled Fusion and Plasma Heating,1988. Europhys. Conf. Abstracts, Vol 12B, Part 1, p139.

[4] A Boileau et al, " The Deduction of Low-Z Ion Temperature and Densities in the JET Tokamak using Charge-Exchange Recombination Spectroscopy", JET-P(87)44.

[5] A Boileau et al, "Observation of Motional Stark Features in the Balmer Spectrum of Deuterium in the JET Plasma", J. Phys. B 22 (1989) L145.

[6] M von Hellerman et al, "Local Measurement of Z_{eff} and Magnetic Fields", to be published.

[7] O N Jarvis et al, Nuclear Fusion 27 (1987) 1755.

[8] M J Loughlin, Ph.D Thesis, University of Birmingham. Harwell Laboratory Report HL88/1382.

[9] S Conroy et al, "Time-Resolved Measurements of Triton Burnup in JET Plasmas", Nuclear Fusion 28 (1988) 2127.

10] P van Belle and G Sadler, in Basic and Advanced Diagnostic Techniques for Fusion Plasmas (Proc Course and Workshop, Varenna 1986), Vol III, Rep EUR 10797 EN, CEC (1987) 767.

[11] M Keilhacker, Plasma Physics and Controlled Fusion 29 (1987) 1401.

[12] D.Veron, Workshop on "Diagnostics for Fusion Reactor Conditions", Varenna, Italy, EUR 8351-II-EN, 1982, Commission of the European Communities, Brussels, Vol.2, p.283.

[13] C Gowers, "The JET Lidar Thomson Scattering System", in JET-P(86)45.

[14] O N Jarvis et al, Rev Sci Instr 57 (1986) 1717.

[15] R Bartiromo et al, "The JET High Resolution Bent Crystal Spectrometer", JET-P(88)11.

[16] R Bartiromo et al, Rev Sci Instr 58 (1987) 788.

[17] J M Adams et al, 16th European Conference on Controlled Fusion and Plasma Heating, 1989. Europhys. Conf. Abstracts, Vol 13B, Part 1, p 63.

[18] T Elevant et al, Bull Am Phys Soc 32 (1987) 1870.

[19] R J Goldston et al, J Comput Phys 43 (1981) 61.

[20] M Pillon et al, "Calibration of Neutron Yield Activation Measurements at JET", JET-P(88)10.

[21] S Conroy, 16th European Conference on Controlled Fusion and Plasma Heating, 1989. Europhys. Conf. Abstracts, Vol 13B, Part 1, p 67.

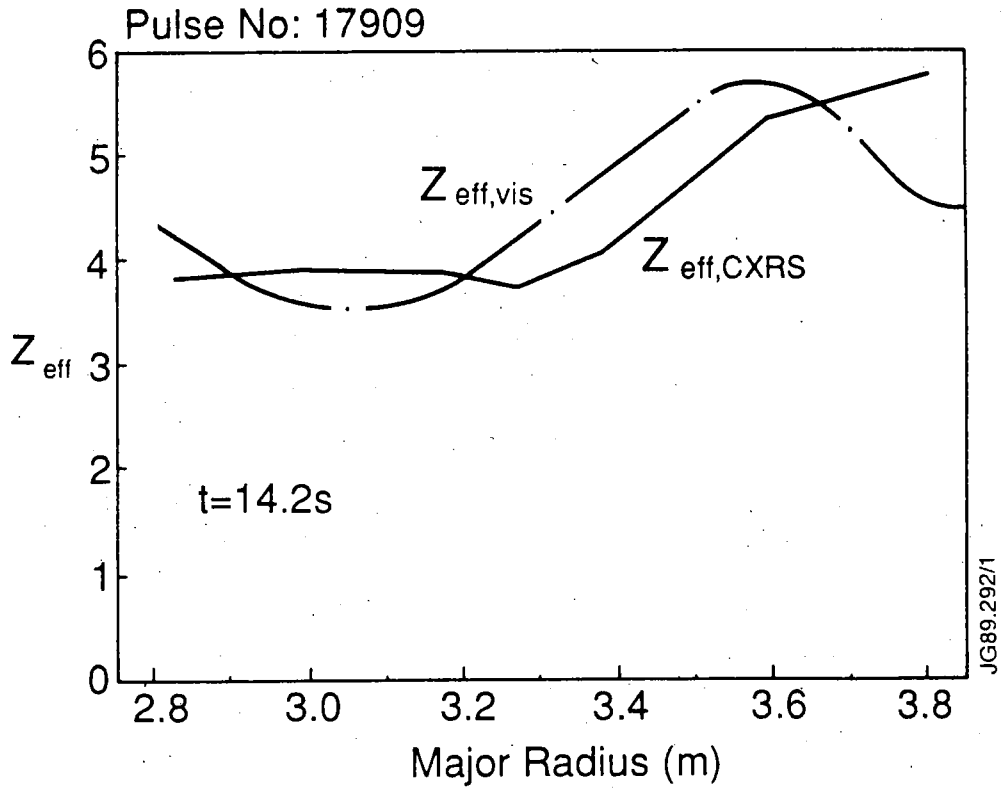

Fig. 1 Comparison of a Z_{eff} profile deduced from Abel-inverted visible bremsstrahlung measurements with the CXRS profile derived from the carbon density measurements. An X-point discharge is illustrated. The plasma centre lies at 3.0m.

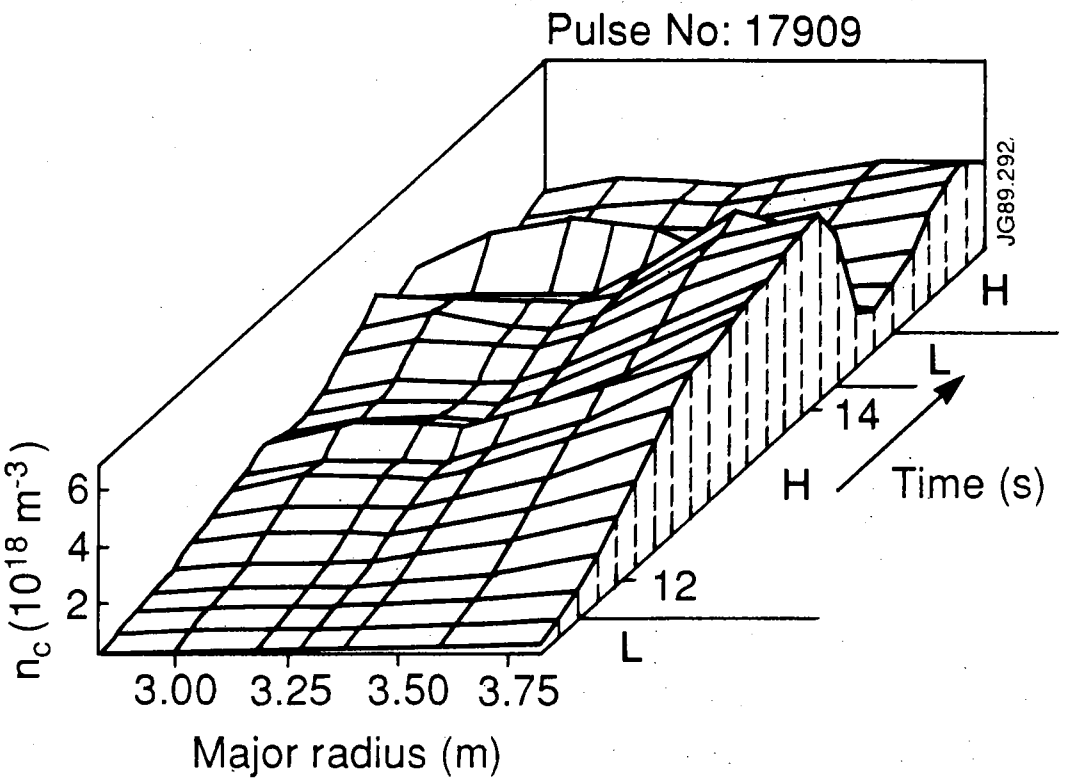

Fig. 2 Showing carbon density profiles obtained from CXRS as a function of time during an X-point discharge; the changes from flat L-mode to hollow H-mode conditions are clearly seen. The plasma centre lies at 3.0m.

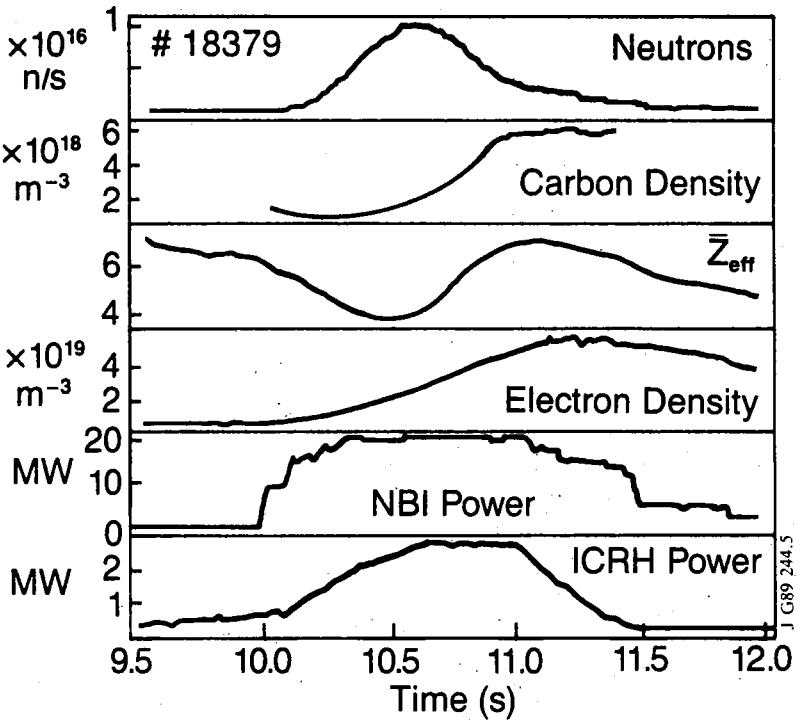

Fig. 3 Illustrating the 'carbon catastrophe' for a low density, high beam power, discharge run on the inner wall. The build-up of impurity carbon in the centre of the discharge abruptly terminates the rise in the total neutron emission strength and creates a narrow peak where otherwise a flat-top (if not a further increase) would have been expected. The periods of application of neutral beam and radiofrequency heating power are also indicated.

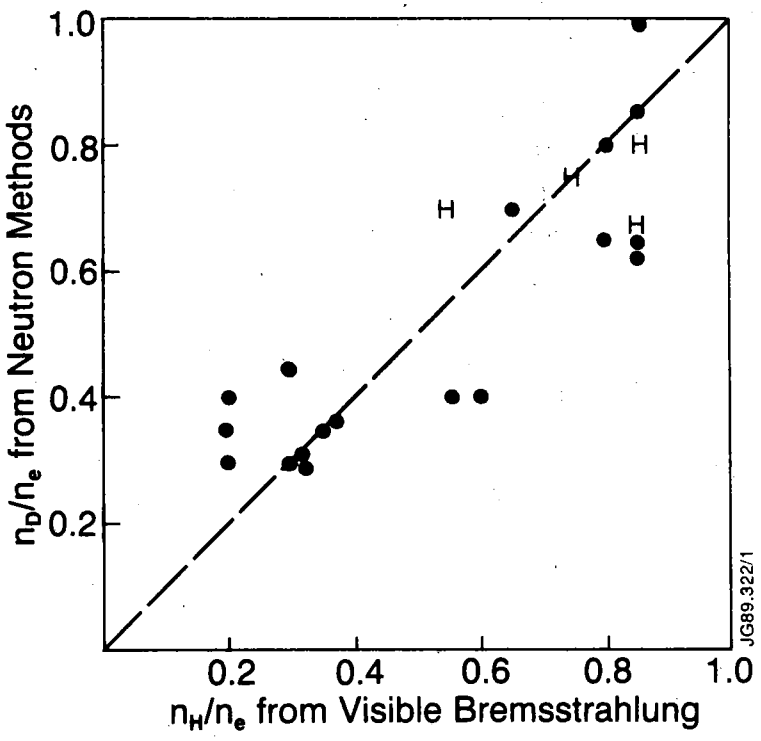

Fig. 4 Comparison of deuterium concentration from neutron measurements with estimates from Z_{eff} data. The values plotted correspond to the plasma centre; the neutron emission profile weighted values may be significantly lower in the case of H-mode plasmas (labelled H).

TABLE I. Attributes of the Measurement Techniques Exploited

Technique	Accuracy	Sampling
Measurement of Z_{eff}		
Visible Bremsstrahlung	± 30%	Line
Plasma Resistivity	± 25%	Axial
Pulse Height Analysis	± 50%	Axial
Charge-Exchange (CXRS)	± 30%	Local
Measurement of n_D/n_e		
Neutron Emission Profiles	± 20%	Axial
Neutron Energy Spectra	± 25%	Axial
NBI Transient Analysis	± 20%	Volume
Triton Burnup	± 20%	Volume

TABLE II. Key Parameters for the Discharges Selected for Study

Discharge		P_{RF}	P_{NBI}	$n_e(0)$	$T_e(0)$	$T_i(0)$	neutrons
Class	No.	(MW)	(MW)	($10^{19}m^{-3}$)	(keV)	(keV)	($10^{15}s^{-1}$)
6 and 7 MA	17793	-	-	4.1	3.0	3.5	0.03
Ohmic	17796	-	-	3.9	3.2	2.9	0.02
^{4}He prefill	17797	-	-	4.1	4.0	4.2	0.04
3 MA	17836	9.6	2.7	3.4	8.8	6.6	0.6
High T_e	17838	11.8	2.6	4.0	8.8	6.4	0.6
5 MA	16370	1.1	8.6	5.7	5.2	7.2	1.3
Combined htg.	16382	6.8	12.0	5.5	7.3	7.4	2.7
3 MA	16041	0.5	8.0	3.4	5.9	10.9	1.9
High T_i	16066	7.9	7.4	3.0	10.0	13.3	3.8
	18379	2.7	19.9	3.1	8.1	15.3	8.3
	18589	1.4	15.2	5.2	5.7	11.0	3.1
3 MA	15894	-	7.5	5.6	5.5	5.3	2.2
H-mode	16259	-	11.5	4.2	6.0	6.7	3.3
	16268	-	13.4	7.3	6.6	7.0	3.7
	18757	-	10.2	2.8	6.8	13.1	3.6
3 MA	16211	7.1	-	5.8	7.8	7.9	1.2
Pellets	16228	10.0	-	5.2	7.7	7.3	1.8
	16235	10.1	6.6	5.6	7.9	8:2	4.3
	17279	7.2	2.8	5.2	8.2	7.4	1.8
5 MA	15182	-	-	4.0	3.7	2.2	3.6
Conditioned	15190	10.2	-	6.6	5.8	5.8	0.8
Vessel	15196	12.1	-	7.1	5.3	5.0	0.8

TABLE III. Axial and Line-Averaged Values for the Effective Charge

Discharge		$Z_{eff}(0)$				$\langle Z_{eff} \rangle$	
Class	No.	Resist.	PHA	CXRS	Vis.br.	CXRS	Vis.br.
6 and 7 MA	17793	3.8	5.0	-	4.6	-	3.4
Ohmic	17796	3.8	4.9	-	4.9	-	3.4
^{4}He prefill	17797	4.1	6.0	-	4.6	-	3.6
3 MA	17836	-	5.2	4.7	4.8	-	3.9
High T_e	17838	-	4.6	6.0	5.4	4.1	4.2
5 MA	16370	4.0	4.7		3.3	-	3.2
Combined htg.	16382	-	5.2	5.4	4.0	-	3.5
3 MA	16041	2.8	4.0	-	3.5	-	2.4
High T_i	16066	-	5.0	5.0	5.2	3.2	3.5
	18379	-	6.5	5.5	-	3.6	4.5
	18589	-	3.5	5.3	-	3.7	3.8
3 MA	15894	-	-	-	1.9	-	1.9
H-mode	16259	-	1.6	1.7	2.1	-	1.8
	16268	-	2.8	2.4	2.4	-	2.3
	18757	-	4.0	4.2	3.0	3.1	3.4
3 MA	16211	-	3.5	-	1.7	-	2.2
Pellets	16228	-	3.0	-	1.7	-	2.1
	16235	-	3.0	-	1.9	-	2.4
	17279	-	-	3.5	2.3	2.8	2.5
5 MA	15182	-	-	-		-	2.1
Conditioned	15190	-	-	-		-	2.0
Vessel	15196	-	-	-		-	1.9

TABLE IV. Comparison of n_D/n_e Values from Neutron Measurements with Values Derived from the Effective Charge.

Discharge		n_H/n_e	n_D/n_e from neutrons			
Class	No.	Eff.Chge	Spectra+ Profiles	NI Trans Analysis	Triton Burnup	Averaged
6 and 7 MA	17793	0.35	0.3	-	0.4	0.35
Ohmic	17796	0.3	0.3	-	0.35	0.3
^{4}He prefill	17797	0.35	0.3	-	0.4	0.35
3 MA	17836	0.3	0.4	-	0.25	0.3
High T_e	17838	0.2	0.35	-	0.25	0.3
5 MA	16370	0.6	0.4	-	0.4	0.4
Combined htg.	16382	0.3	0.35	-	0.3	0.3
3 MA	16041	0.55	0.35	0.4	0.4	0.4
High T_i	16066	0.30	≤0.5	0.45	-	0.45
	18379	0.20		0.35	-	0.35
	18589	0.20		0.4	0.4	0.4
3 MA	15894	0.85	0.65	0.60	0.55	
H-mode	16259	0.85	0.8	0.4	0.55	
	16268	0.75	0.75	0.30	0.45	
	18757	0.55	0.7	0.5	-	
3 MA	16211	0.85	0.85	-	-	0.85
Pellets	16228	0.85	1.0	-	-	1.0
	16235	0.85	0.65	-	-	0.65
	17279	0.65	0.7	-	-	0.7
5 MA	15182	0.8	0.8	-	-	0.8
Conditioned	15190	0.8	0.65	-	-	0.65
Vessel	15196	0.85	0.65	-	-	0.65

N.B. The H-mode discharges form a special case as they may have hollow density, Z_{eff} and neutron emission profiles.